Structural Engineering and Mechanics, *Vol. 46, No. 5 (2013) 645-672*
DOI: http://dx.doi.org/10.12989/sem.2013.46.5.645

Seismic analysis of frame-strap footing-nonlinear soil system to study column forces

Vivek Garg[*1] and Manjeet S. Hora[2b]

[1]*Department of Civil Engineering, Maulana Azad National Institute of Technology, Bhopal, India*
[2]*Department of Applied Mechanics, Maulana Azad National Institute of Technology, Bhopal, India*

(Received November 7, 2012, Revised April 11, 2013, Accepted April 25, 2013)

Abstract. The differential settlements and rotations among footings cannot be avoided when the frame-footing-soil system is subjected to seismic/dynamic loading. Also, there may be a situation where column(s) of a building are located near adjoining property line causes eccentric loading on foundation system. The strap beams may be provided to control the rotation of the footings within permissible limits caused due to such eccentric loading. In the present work, the seismic interaction analysis of a three-bay three-storey, space frame-footing-strap beam-soil system is carried out to investigate the interaction behavior using finite element software (ANSYS). The RCC structure and their foundation are assumed to behave in linear manner while the supporting soil mass is treated as nonlinear elastic material. The seismic interaction analyses of space frame-isolated footing-soil and space frame-strap footing-soil systems are carried out to evaluate the forces in the columns. The results indicate that the bending moments of very high magnitude are induced at column bases resting on eccentric footing of frame-isolated footing-soil interaction system. However, use of strap beams controls these moments quite effectively. The soil-structure interaction effect causes significant redistribution of column forces compared to non-interaction analysis. The axial forces in the columns are distributed more uniformly when the interaction effects are considered in the analysis.

Keywords: seismic loading; nonlinear soil; soil-structure interaction; strap footing; space frame; isolated footing

1. Introduction

In a design process, footings can be proportioned for uniform settlements for a particular load combination only. However, load on frame-footing-soil system may be dynamic in nature and subjected to different load combinations. This results in differential settlements and rotations of foundation system particularly for the structures resting on highly compressible soils. These displacements along with stiffness of the frame cause redistribution of forces/stresses in the frame members. But in actual practice the influence of the displacements induced in supporting soil media on the structural behavior of the super-structure is usually ignored to simply the analysis. A more rational solution of a soil-structure interaction problem can be achieved by appropriate analysis.

∗Corresponding author, Assistant Professor, E-mail: vivek_garg5@yahoo.co.in
[a]Professor, E-mail: hora1961@gmail.com

http://www.techno-press.org/?journal=sem&subpage=8 ISSN: 1225-4568 (Print), 1598-6217 (Online)

A strap (or cantilever) footing may be provided when one or more columns exist on the common property line. It comprises of two or more footings of individual columns, connected by a beam called strap beam. The strap beam transmits the moment caused by eccentricity of load on the external column footing to the interior column footing. The strap beam must be sufficiently rigid to control the rotation of eccentric footing. This type of footing is found more suitable when there are heavy loads on adjoining footings and no overlapping exists between their areas.

Numerous investigators emphasized to consider the effect of soil-structure interaction in the design process. They have quantified the effect of interaction behaviour and established that there is redistribution of forces in the frame members.

Masonry infill walls confined by reinforced concrete frames on all four sides play a vital role in resisting the lateral seismic loads on buildings. An extensive review of the research on testing and modeling of masonry-infilled frames is reported by Moghaddam and Dowling (1987).

Viladkar *et al*. (1994) presented a new approach for the physical and material modelling of a space frame-raft-soil system. The beams and columns of the superstructure is discretized by a modified Timoshenko beam bending element with six degrees of freedom per node and structural slabs and raft are discretized by a modified Mindlin's plate bending element with five degrees of freedom per node. The soil media is represented by the coupled finite-infinite elements with three degrees of freedom per node. The constitutive modelling involves the use of the hyperbolic model to account for the soil nonlinearity. They compared the behaviour of the space frame-raft-soil system under the linear and nonlinear interaction.

A computational iterative scheme for studying the effect of soil-structure interaction on axial force and column moments is presented by Mandal *et al*. (1998). The results obtained from the computational scheme were validated from experimental study. A small scale two-storey two-bay frame made of perspex was analysed. The frame was placed on a kaolin bed with adequate arrangement of drainage. The proposed computational scheme could be used to predict increase in axial force and moments in structural members due to the effect of soil-structure interaction.

An idealized 2-dimensional plane strain seismic soil-structure interaction analysis based on a substructure method is presented by Kutanis and Elmas (2001). To investigate the interaction effect non-interaction analysis and linear and nonlinear analyses were performed. Computations were made by taking different peak acceleration and shear wave velocity. The soil plasticity was modelled with the Von Mises failure criteria.

Asteris (2003) proposed a new finite element technique for the analysis of brickwork infilled plane frame subjected to lateral loading. He investigated the influence of the masonry infill panel opening in the reduction of the infilled frame stiffness. A parametric study was carried out considering the position and percentage of masonry infill panel opening. It is found that the presence of infill causes decrease in shear forces on the frame columns except on columns of soft ground storey.

Three-dimensional finite element analysis in time domain on dynamic soil-pile-structure interaction of a tall building is carried out by Lu *et al*. (2003). The viscous boundary of soil is implemented in general-purpose finite element program (ANSYS) used in the analysis. The influences of parameters, such as soil property, excitation, buried depth and the rigidity of the structure, on dynamic characteristics, seismic response and interaction effect of soil-structure interaction system are discussed.

Roy *et al*. (2005) performed an analysis on an idealized model consisting of multi-storey 3-D frame structure with grid foundation. The grid foundation is assumed to rest on springs, which idealize the soil behaviour.

Hora (2006) presented the computational methodology adopted for nonlinear soil-structure interaction analysis of infilled frame-foundation-soil system. The unbounded domain of the soil mass has been discretized with coupled finite-infinite elements to achieve computational economy. The nonlinear behaviour of the soil mass was modelled using hyperbolic model. The incremental-iterative nonlinear solution algorithm was adopted for carrying out the nonlinear elastic interaction analysis. The interaction analysis showed that the nonlinearity of soil mass plays an important role in redistribution of forces in the superstructure.

The effect of soil flexibility on base shear and uncoupled torsional-to-lateral natural period ratio is examined by Bhattacharya *et al*. (2006). The results of the study conclude that the effect of soil-structure interaction may cause considerable increase in seismic base shear of low-rise building frames, particularly those with isolated footings.

The influence of column spacing on the behavior of a space frame-raft-soil system under static load is studied by Nataralan and Vidivelli (2009). The analyses were carried out for linear and non-linear cases, in which soil was treated as a homogeneous and isotropic continuum. Settlement was greater in the non-linear analysis and the settlements were higher for higher column spacing. Contact pressure distribution was more uniform in the non-linear case and its magnitude was less than that of linear soil, particularly in the end panels of the raft.

The effect of contact between strap beam and bearing stratum is studied by Guzman (2010). The results indicate that when a strap footing is used as part of a foundation system, a detail that allow for pressure to be relieved from the strap beam is necessary on construction documents. Without it, a considerable unforeseen load path could be created that may result in the failure of strap beam followed by overstress of the soil under the eccentric footing.

The interaction and non-interaction analyses for the space frame-raft foundation-soil system using ANSYS finite element code is compared by Thangaraj and Ilamparuthi (2010). The soil was treated as an isotropic, homogenous and elastic half space medium. A detailed parametric study was conducted by varying the soil and raft stiffness for a constant building stiffness. The interaction analysis showed less total and differential settlements than the non-interaction analysis and relative stiffness of soil plays major role in the performance of the raft.

The effects of horizontal stresses and horizontal displacements in loaded raft foundation are studied by Swamy Rajashekhar *et al*. (2011). The numerical experiments are performed on three dimensional mathematical models. The results of uncoupled analysis i.e., complete slip/frictionless interface between foundation and soil and the coupled analysis i.e., complete welding/bonding of joints between foundation and soil elements were compared with the results of non-interactive analysis. They concluded that the response of the structure does change in soil-structure-interaction analysis when compared to non-interactive analysis but member end actions for beams and columns are almost same in coupled and uncoupled analysis.

The principles of elasto/viscoplastic finite element analysis are presented by Abdullah (2011). Plasticity models such as Drucker-Prager, Von-Mises, Tresca and Mohr-Coulomb models with associated and non-associated flow rules were incorporated in the viscoplastic algorithm. The ultimate bearing capacity of a rigid surface footing resting on weightless clayey soil predicted by Tresca model agrees very well with that obtained by Prandtl exact solution.

Asteris *et al*. (2011) presented a general review of the different macromodels used for the analysis of infilled frames by various researchers from time to time. The studies in the field of analysis of infilled frames stressed that the numerical simulation of infilled frames is difficult and generally unreliable because of very large number of parameters to be taken into account and the magnitude of the uncertainties associated with most of them. The advantages and disadvantages of each macromodel with practical recommendations for the implementation of the model are highlighted.

Asteris and Cotsovos (2012) investigated the effect of un-reinforced concrete or masonry infill walls on the overall structural response of reinforced concrete frames under static monotonic and seismic loading. The effect of infill walls on structural stiffness, load-carrying capacity, deformation profile, cracking, ductility and mode of failure of the frame was also studied.

The important contribution of infill walls in the resistance of earthquake loads along with a presentation of the behavior modes of the infill and the bounding frame is documented by Chrysostomou and Asteris (2012). Recommendations are made for the in-plane material properties, failure modes, strength and stiffness as well as deformation characteristics of infilled frames.

The interaction effect of frame, isolated footing and soil media under seismic loading is studied by Agrawal and Hora (2012). Various analyses are performed on frame-footing-soil system by considering plane frame, infill frame, homogeneous soil and layered soil mass. The frame is considered to act in linear elastic manner while the soil mass to act as nonlinear elastic manner. They concluded that the shear forces and bending moments in superstructure get significantly altered due to differential settlements of the soil mass.

Agrawal and Hora (2012) analysed the infilled building frame-isolated footing-soil system under seismic loading. The well known hyperbolic soil model is used to account for the nonlinearity of the soil mass whereas material of the frame, infill, column and footing is assumed to follow the linear stress-strain relationship. The coupled isoparametric finite-infinite elements are used for modeling of the interaction system. The inclusion of infill wall significantly increases the stiffness of the frame which in turn reduces the forces in columns and beams.

Thangaraj and Ilamparuthi (2012) analysed the space frame-mat foundation-soil system as a single compatible unit. The relative stiffness factors which are the function of the modulus of the soil, modulus of frame raft materials and geometric properties of the structural elements are used to examine the interaction behavior.

2. Problem for investigation

The interaction effect of a 3 bay × 3 bay three-storey RCC space frame founded on strap footing and resting on homogeneous soil mass is analyzed under seismic loading in the present problem. The problem under consideration is symmetric about one axis in terms of geometry, material properties and loading. Hence, to make the model computationally economical only half of the model is considered for analysis. To investigate the interaction behavior, the interaction analyses are carried out for the three cases. Case-1 is the conventional non-interaction analysis (NIA) considering the columns fixed at their bases. Case-2 is the nonlinear interaction analysis of space frame-isolated footing-soil system (NLIA-ISO) considering the columns supported on individual column footings and resting on soil media. Case-3 is the nonlinear interaction analysis of space frame-strap footing-soil system (NLIA-STR) considering the individual footings of Case-2 connected by strap beams.

The RCC structure and their foundation are assumed to behave in linear manner while the supporting soil mass is treated as nonlinear elastic material. The frame-foundation-soil system is considered to act as a single compatible structural unit for more realistic analysis.

The seismic forces have been calculated by static method as per Bureau of Indian standards

Table 1 Parameters/data used for the analysis of problem

Sr. No.	Description	Value/type
1.	Number of bays in X direction	3
2.	Number of bays in Y direction	3
3.	Number of storeys	3
4.	Storey height	3.5 m
5.	Column height below plinth beam	2.0 m
6.	Bay width in X direction	6.0 m
7.	Bay width in Y direction	6.0 m
8.	Size of columns	0.4 m × 0.4 m
9.	Size of plinth and floor beams	0.3 m × 0.5 m
10.	Size of strap beams	0.4 m × 1.1 m
11.	Thickness of roof slabs	0.15 m
12.	Isolated footing size	2 m × 2 m × 0.5 m
13.	Elastic modulus of concrete	2.5×10^7 kN/m^2
14.	Poisson's ratio of concrete	0.15
15.	Extent of soil mass	200 m × 100 m × 90 m
16.	Initial tangent modulus of soil	1.47×10^4 kN/m^2
17.	Poisson's ratio of soil	0.35
18.	Seismic zone	V
19.	Seismic intensity	Very severe
20.	Zone factor	0.36
21.	Importance factor	1
22.	Building frame system	Ordinary RC moment-resisting frame
23.	Response Reduction Factor	3
24.	Spectral acceleration coefficient	2.5

code IS 1893 (Part 1): 2002. The parameters/data used for the analysis of problem are given in Table 1.

The seismic forces have been evaluated by equivalent static force method. The brick infill walls are considered as non-structural element in the present analysis and ignore its interaction with the bounding frame. A step-by-step procedure as per Bureau of Indian standards code IS 1893 (Part 1):2002 is as follows:

(i) Calculation of lumped masses to various floor levels

The earthquake forces are calculated for the full dead load plus the percentage of imposed load as per IS 1893 (Part 1): 2002. While computing the seismic weight of each floor, the weight of columns and walls in any storey are equally distributed to the floors above and below the storey. The seismic weight of the whole building is the sum of the seismic weights of all the floors.

(ii) Determination of fundamental natural period

The approximate fundamental natural period of vibration (T_a), in seconds, of a moment-resisting frame building without brick infill panels for RC frame building are estimated by the empirical expression

$$T_a = 0.075h^{0.75} \tag{1}$$

where

h = Height of building in meter

(iii) Determination of design horizontal seismic coefficient

The design horizontal seismic coefficient A_h for a structure is determined by the following expression

$$A_h = \frac{Z\ I\ S_a}{2\ R\ g} \tag{2}$$

where,

Z = Zone factor for the maximum considered earthquake (MCE) and service life of structure in a zone

I = Importance factor

R = Response reduction factor

$\frac{S_a}{g}$ = Average response acceleration coefficient

(iv) Determination of design base shear

The total design lateral force or design seismic base shear (V_b) along any principal direction is determined by the following expression

$$V_b = A_h W \tag{3}$$

where,

A_h = Design horizontal seismic coefficient

W = Seismic weight of the building

(v) Distribution of base shear

The design base shear (V_b) is distributed along the height of building as per the following expression

$$Q_i = V_b \frac{W_i h_i^2}{\sum_{j=1}^{n} W_j h_j^2} \tag{4}$$

Table 2 Gravity and seismic loads on superstructure

Sr. No.	Loads	Structural component	Intensity
1	Gravity loads which include self weight and imposed load on beams (kN/m)	Plinth beams	
		(i) Peripheral beams	19.0
		(ii) Other beams	13.0
		Floor beams (1st and 2nd storeys)	
		(i) Peripheral beams	35.0
		(ii) Other beams	45.0
		Floor beams (3rd storey)	
		(i) Peripheral beams	22.0
		(ii) Other beams	29.0
2	Seismic loads at different floor levels (kN)	First floor	
		(i) Outside	32.0
		(ii) Inside	47.0
		Second floor	
		(i) Outside	127.0
		(ii) Inside	186.0
		Third floor	
		(i) Outside	230.0
		(ii) Inside	315.0

where,

Q_i = Design lateral force at floor 'i'
W_i = Seismic weight of floor 'i'
h_i = Height of floor 'i' measured from base
n = Number of storeys in the building

The imposed load is considered 1.5 kN/m^2 (25% of imposed load is considered to calculate seismic weight) on roof and 4.0 kN/m^2 (50% of imposed load is considered to calculate seismic weight) on other floors. The thickness of brick wall is considered 230 mm in peripheral walls and 130 mm in other walls. The evaluated uniformly distributed loads are applied on floor and plinth beams which include self weight and imposed load and the estimated seismic loads applied at different floor levels on the superstructure are shown in Table 2.

The superstructure of proposed model is depicted in Fig. 1.

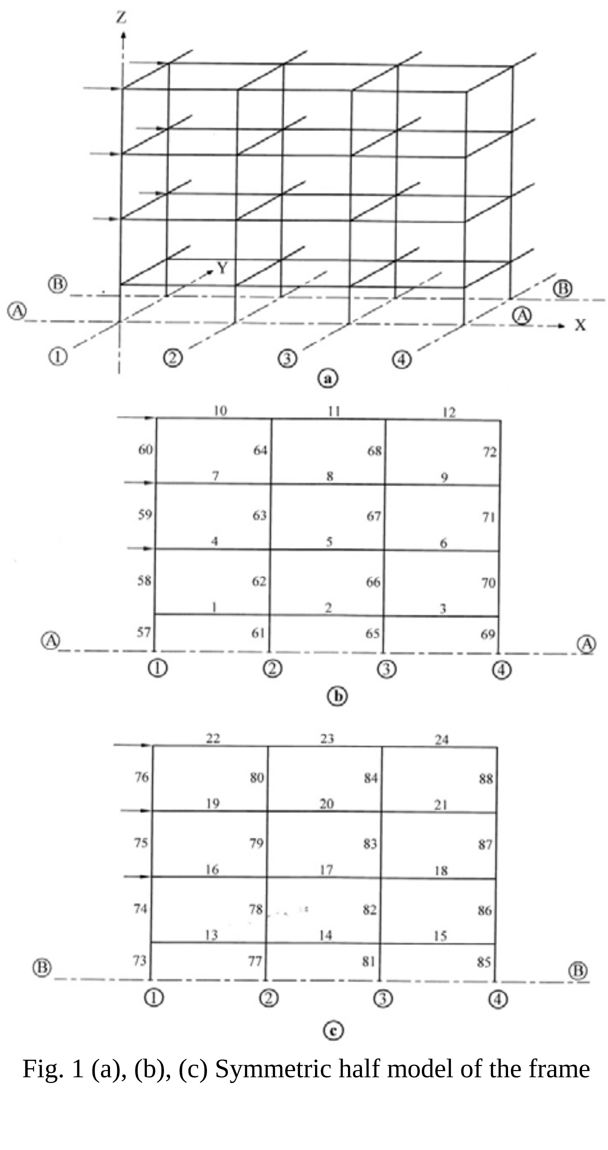

Fig. 1 (a), (b), (c) Symmetric half model of the frame

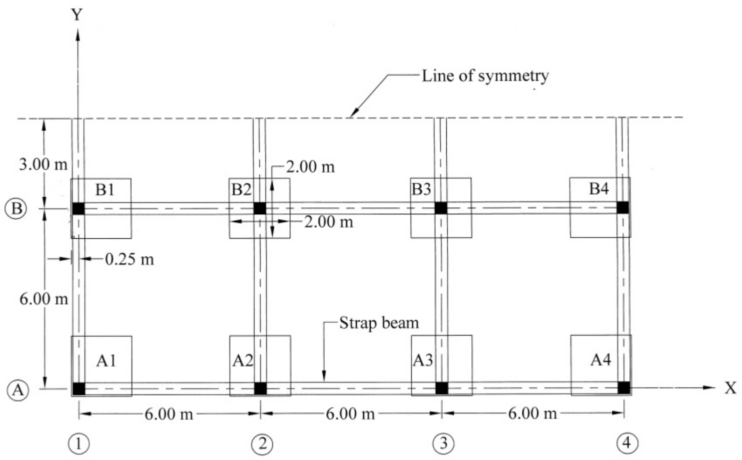

Fig. 2 Symmetric half model of foundation plan

Table 3 Description of elements used for finite element analysis

Sr. No.	Component	Element	No. of Nodes	Degree of freedom per node
1	Space frame and strap beams	BEAM4	2	Six degrees of freedom per node (Ux, Uy, Uz, Rx, Ry, and Rz)
2	Roof slab	SHELL181	4	Six degrees of freedom per node (Ux, Uy, Uz, Rx, Ry, and Rz)
3	Footing	SHELL281	8	Six degrees of freedom per node (Ux, Uy, Uz, Rx, Ry, and Rz)
4	Soil	SOLID92	10	Three degrees of freedom per node (Ux, Uy, Uz)
5	Interface at footing surface	CONTA174	8	Six degrees of freedom per node (Ux, Uy, Uz, Rx, Ry, and Rz)
6	Interface at soil surface	TARGE170	6	Three degrees of freedom per node (Ux, Uy, Uz)

The symmetric half model of foundation plan is depicted in Fig. 2.

3. Finite element modeling

The non-interaction and nonlinear interaction analyses of the problem are carried out using the general-purpose finite element software (ANSYS). Various elements used for the analysis are depicted in Table 3.

The surface-to-surface contact between interface of footing and soil is defined by internal multipoint constraint (MPC) approach. For shell-solid assembly the contact surface pastes onto shell element faces and the target surfaces paste onto solid element faces. The interface characteristics between the footing and soil are represented by CONTA174 and TARGE170 elements. CONTA174 is a 3-D, 8-node, higher order quardrilateral element which can be used to represent surface-to-surface contact between 3-D target surfaces (TARGE170) and a deformable surface defined by this element. This element may be located on the surfaces of shell elements with mid-side nodes. It has the same geometric characteristics as the shell element face with which it is connected. TARGE170 is used to represent various 3-D target surfaces for the associated contact elements. This target surface is discretized by a set of target segment elements (TARGE170) and is paired with its associated contact surface via a shared real constant set. For flexible targets, these elements may overlay the solid elements (SOLID92) describing the boundary of the deformable target body.

The element size for beams, columns, slabs and footings are taken as 0.25 m. The soil mass is discretized with finer meshes in close vicinity of footing where stresses are of higher order. It is assumed that the joints between various members are perfectly rigid. The soil mass is idealized as isotropic, homogeneous, half-space model. The semi-infinite extent of the soil model is considered as 200 m × 100 m × 90 m which is achieved by trial and error performing linear analysis. The extent of soil mass is decided where vertical and horizontal stresses are found to be negligible due to loading on the superstructure. The vertical displacements in soil mass are restrained at the bottom boundary whereas horizontal displacements are restrained at vertical boundaries. The finite element discretization of the problem is shown in Fig. 3.

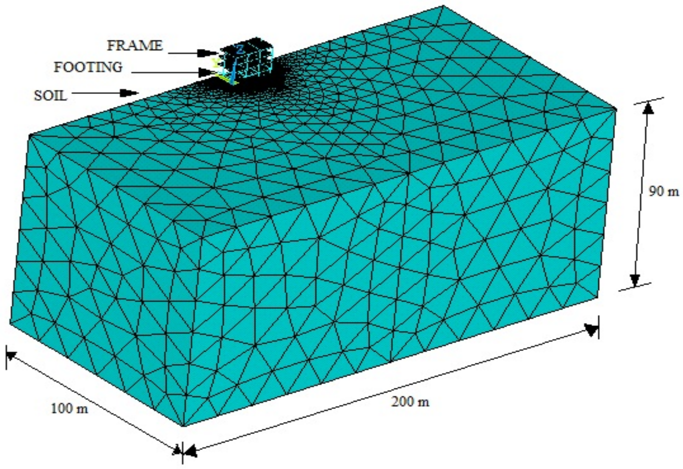

Fig. 3 Finite element discretization of frame-footing-soil system (symmetric half model)

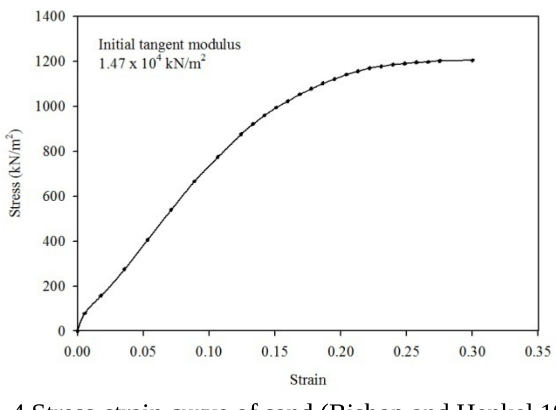

Fig. 4 Stress-strain curve of sand (Bishop and Henkel 1957)

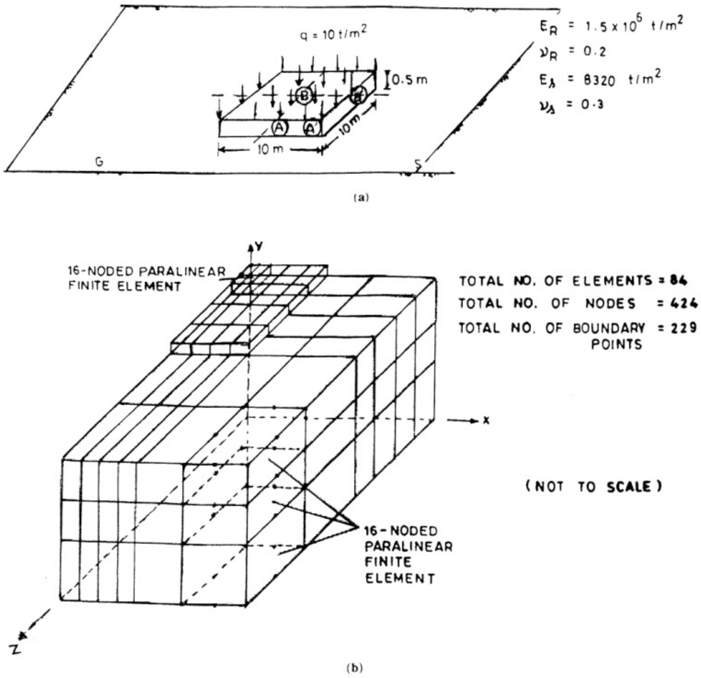

Fig. 5 (a) Square raft resting on soil surface, (b) Three dimensional finite element discretization of quarter portion of raft-soil system (Noorzaei *et al.* 1996)

Table 4 Comparison of total vertical settlement (mm) of central, mid side and corner of the raft

Location	Present Study	Noorzaei *et al.* 1996	Buragohain *et al.* 1979
Center of raft	10.492	9.937	10.470
Mid-side of raft	7.288	7.389	7.250
Corner of raft	4.654	5.486	4.580

The nonlinear stress-strain curve of sandy soil (Bishop and Henkel 1957) is considered for the nonlinear analysis as shown in Fig. 4. The nonlinear parameters of this soil are adopted in the present analysis.

4. Validation of results

The results obtained by the ANSYS software are validated with the results already available in the literature (Noorzaei *et al.* 1996, Buragohain *et al.* 1979). They carried out the interaction analysis of a square raft (10 m × 10 m × 0.5 m) resting on soil mass. The raft is subjected to uniform pressure of 100 kN/m^2. The geometry, material properties, loading and element discretization of the square raft is shown in Fig. 5.

The comparison of total settlement (mm) of central, mid side and corner of the raft is provided in Table 4.

Table 5 Comparison of total vertical settlement *Uz* (mm) of footings for various analyses

Footing No.	Co-ordinates			Case-2 NLIA-ISO	Case-3 NLIA-STR	Comparison of interaction analyses
	X	Y	Z	2	3	3/2
A1	0.0	0.0	0.0	-40.91	-40.87	1.00
A2	6.0	0.0	0.0	-65.79	-56.09	0.85
A3	12.0	0.0	0.0	-74.69	-63.67	0.85
A4	18.0	0.0	0.0	-83.28	-70.58	0.85
B1	0.0	6.0	0.0	-49.21	-45.54	0.93
B2	6.0	6.0	0.0	-75.01	-61.56	0.82
B3	12.0	6.0	0.0	-83.95	-68.84	0.82
B4	18.0	6.0	0.0	-91.17	-74.29	0.81

Note- Negative sign indicates downward displacement
3/2 indicates ratio of the total settlement Case-3/Case-2

5. Interaction analysis

In the present analysis the total load on the structure is applied in ten equal load increments. The incremental iterative technique is used for nonlinear interaction analysis. The axial force and bending moments in columns are found to vary nonlinearly with load increments. The forces in columns are evaluated due to non-interaction analysis (NIA) and nonlinear interaction analyses (NLIA) and discussed subsequently.

5.1 Total vertical settlement of footings

The total settlement of footings frame-footing-soil system due to various analyses is depicted in Table 5 for the total load on the structure.

5.1.1 Effect of inclusion of strap beam

Comparison between NLIA-ISO and NLIA-STR

The comparison of total settlement due to NLIA-ISO and NLIA-STR reveals that the strap beam causes decrease in the footing settlement. NLIA-STR provides variation of 0.81 to 1.00 times in the vertical settlement compared to NLIA-ISO. The maximum decrease of nearly 0.81 times is found in the side column footing (footings B4) whereas the ratio of nearly 1.00 times is found in the corner column footing (footings A1). The maximum vertical settlement of nearly 91.17 mm is found in side footing B4 of NLIA-ISO. This value of vertical settlement becomes almost 0.81 times in case of NLIA-STR.

5.2 Axial force (Fz) in the columns

The axial force (*Fz*) in the columns of frame-footing-soil system due to various analyses is depicted in Tables 6-7 for the total load on the structure.

Table 6 Comparison of axial force *Fz* (kN) in columns for various analyses (*y* = 0 m)

Member No.	Co-ordinates			Case-1 NIA	Case-2 NLIA-ISO	Case-3 NLIA-STR	Comparison of interaction analyses		
	X	Y	Z	1	2	3	2/1	3/1	3/2
57	0.0	0.0	0.0	-360.59	-566.10	-487.57	1.57	1.35	0.86
57	0.0	0.0	2.0	360.59	566.10	487.57	1.57	1.35	0.86
58	0.0	0.0	2.0	-344.79	-520.22	-437.35	1.51	1.27	0.84
58	0.0	0.0	5.5	344.79	520.22	437.35	1.51	1.27	0.84
59	0.0	0.0	5.5	-230.19	-346.47	-290.43	1.51	1.26	0.84
59	0.0	0.0	9.0	230.19	346.47	290.43	1.51	1.26	0.84
60	0.0	0.0	9.0	-93.44	-142.07	-118.59	1.52	1.27	0.83
60	0.0	0.0	12.5	93.44	142.07	118.59	1.52	1.27	0.83
61	6.0	0.0	0.0	-1080.60	-995.16	-1048.90	0.92	0.97	1.05
61	6.0	0.0	2.0	1080.60	995.17	1048.90	0.92	0.97	1.05
62	6.0	0.0	2.0	-938.17	-862.16	-916.75	0.92	0.98	1.06
62	6.0	0.0	5.5	938.17	862.16	916.75	0.92	0.98	1.06
63	6.0	0.0	5.5	-578.85	-531.02	-564.38	0.92	0.98	1.06
63	6.0	0.0	9.0	578.85	531.02	564.38	0.92	0.98	1.06
64	6.0	0.0	9.0	-224.19	-201.45	-217.13	0.90	0.97	1.08
64	6.0	0.0	12.5	224.19	201.45	217.13	0.90	0.97	1.08
65	12.0	0.0	0.0	-1001.40	-1143.60	-1079.60	1.14	1.08	0.94
65	12.0	0.0	2.0	1001.40	1143.60	1079.60	1.14	1.08	0.94
66	12.0	0.0	2.0	-874.55	-996.64	-933.80	1.14	1.07	0.94
66	12.0	0.0	5.5	874.55	996.64	933.80	1.14	1.07	0.94
67	12.0	0.0	5.5	-546.57	-625.17	-585.53	1.14	1.07	0.94
67	12.0	0.0	9.0	546.57	625.17	585.53	1.14	1.07	0.94
68	12.0	0.0	9.0	-212.23	-248.15	-229.87	1.17	1.08	0.93
68	12.0	0.0	12.5	212.23	248.15	229.87	1.17	1.08	0.93
69	18.0	0.0	0.0	-848.93	-1054.70	-935.00	1.24	1.10	0.89
69	18.0	0.0	2.0	848.93	1054.70	935.00	1.24	1.10	0.89
70	18.0	0.0	2.0	-711.11	-830.89	-771.71	1.17	1.09	0.93
70	18.0	0.0	5.5	711.11	830.89	771.71	1.17	1.09	0.93
71	18.0	0.0	5.5	-425.32	-501.37	-463.00	1.18	1.09	0.92
71	18.0	0.0	9.0	425.32	501.37	463.00	1.18	1.09	0.92
72	18.0	0.0	9.0	-155.46	-184.57	-169.92	1.19	1.09	0.92
72	18.0	0.0	12.5	155.46	184.57	169.92	1.19	1.09	0.92

Note- Negative sign indicates that axial force acts in downward direction

Table 7 Comparison of axial force *Fz* (kN) in columns for various analyses (*y* = 6 m)

Member No.	Co-ordinates			Case-1 NIA	Case-2 NLIA-ISO	Case-3 NLIA-STR	Comparison of interaction analyses		
	X	Y	Z	1	2	3	2/1	3/1	3/2
73	0.0	6.0	0.0	-776.70	-802.29	-803.33	1.03	1.03	1.00
73	0.0	6.0	2.0	776.70	802.29	803.33	1.03	1.03	1.00
74	0.0	6.0	2.0	-703.70	-750.16	-726.58	1.07	1.03	0.97
74	0.0	6.0	5.5	703.70	750.16	726.58	1.07	1.03	0.97
75	0.0	6.0	5.5	-454.58	-488.22	-470.18	1.07	1.03	0.96
75	0.0	6.0	9.0	454.58	488.22	470.18	1.07	1.03	0.96
76	0.0	6.0	9.0	-184.19	-199.35	-191.35	1.08	1.04	0.96
76	0.0	6.0	12.5	184.19	199.35	191.35	1.08	1.04	0.96

Table 7 Continued

77	6.0	6.0	0.0	-1734.80	-1348.80	-1517.40	0.78	0.87	1.13
77	6.0	6.0	2.0	1734.80	1348.80	1517.40	0.78	0.87	1.13
78	6.0	6.0	2.0	-1497.00	-1191.60	-1333.60	0.80	0.89	1.12
78	6.0	6.0	5.5	1497.00	1191.60	1333.60	0.80	0.89	1.12
79	6.0	6.0	5.5	-924.86	-727.50	-819.35	0.79	0.89	1.13
79	6.0	6.0	9.0	924.86	727.50	819.35	0.79	0.89	1.13
80	6.0	6.0	9.0	-364.08	-279.55	-319.10	0.77	0.88	1.14
80	6.0	6.0	12.5	364.08	279.55	319.10	0.77	0.88	1.14
81	12.0	6.0	0.0	-1641.40	-1507.00	-1556.80	0.92	0.95	1.03
81	12.0	6.0	2.0	1641.40	1507.00	1556.80	0.92	0.95	1.03
82	12.0	6.0	2.0	-1419.20	-1340.10	-1357.20	0.94	0.96	1.01
82	12.0	6.0	5.5	1419.20	1340.10	1357.20	0.94	0.96	1.01
83	12.0	6.0	5.5	-885.93	-832.20	-847.29	0.94	0.96	1.02
83	12.0	6.0	9.0	885.93	832.20	847.29	0.94	0.96	1.02
84	12.0	6.0	9.0	-350.61	-332.97	-336.43	0.95	0.96	1.01
84	12.0	6.0	12.5	350.61	332.97	336.43	0.95	0.96	1.01
85	18.0	6.0	0.0	-1303.60	-1330.20	-1319.30	1.02	1.01	0.99
85	18.0	6.0	2.0	1303.60	1330.20	1319.30	1.02	1.01	0.99
86	18.0	6.0	2.0	-1107.40	-1104.20	-1119.00	1.00	1.01	1.01
86	18.0	6.0	5.5	1107.40	1104.20	1119.00	1.00	1.01	1.01
87	18.0	6.0	5.5	-669.70	-664.02	-675.81	0.99	1.01	1.02
87	18.0	6.0	9.0	669.70	664.02	675.81	0.99	1.01	1.02
88	18.0	6.0	9.0	-251.79	-247.87	-253.60	0.98	1.01	1.02
88	18.0	6.0	12.5	251.79	247.87	253.60	0.98	1.01	1.02

Note- Negative sign indicates that axial force acts in downward direction

5.2.1 Effect of soil-structure interaction

The comparison of axial force due to NIA and NLIA reveals that the interaction effect causes significant redistribution of the forces in the columns. The inner columns are relieved of the forces and corresponding increase is found in the corner columns due to interaction effects. This redistribution of axial forces is more significant in case of NLIA-ISO compared to NLIA-STR.

(i) Comparison between NIA and NLIA-ISO

NLIA-ISO provides significant variation of 0.77 to 1.57 times in the axial force compared to NIA. The maximum decrease of nearly 0.77 times is found in the inner column of third storey (member 80) whereas the maximum increase of nearly 1.57 times is found in the corner column below plinth level (member 57). The maximum compressive force of nearly 1734.80 kN is found in the inner column below plinth level (member 77) of NIA. This value of force becomes almost 0.78 times in case of NLIA-ISO.

(ii) Comparison between NIA and NLIA-STR

The significant variation of 0.87 to 1.35 times is found in the axial force due to NLIA-STR compared to NIA. The maximum decrease of nearly 0.87 times is found in the inner column below plinth level (member 77) whereas the maximum increase of nearly 1.35 times is found in the corner column below plinth level (member 57). The maximum compressive force of nearly 1734.80 kN is found in the inner column below plinth level (member 77) of NIA. This value of force becomes almost 0.87 times in case of NLIA-STR.

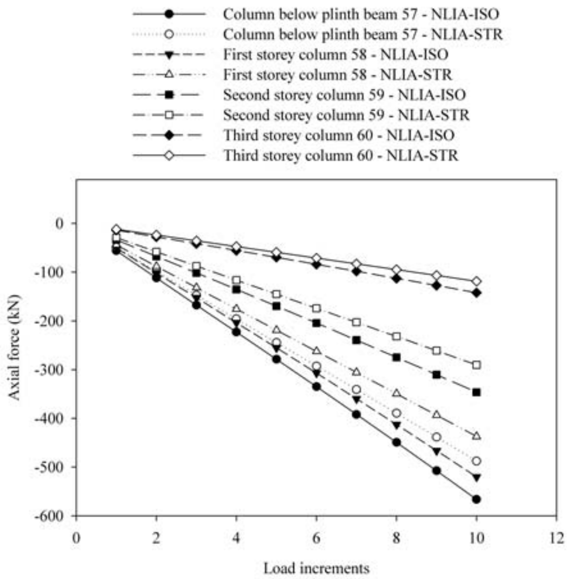

Fig. 6 Comparison of axial force (*Fz*) in corner columns (members 57 to 60)

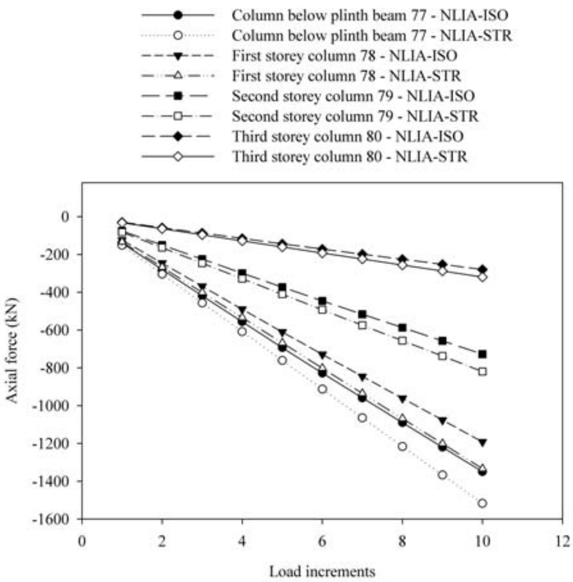

Fig. 7 Comparison of axial force (*Fz*) in inner columns (members 77 to 80)

5.2.2 Effect of inclusion of strap beam

Comparison between NLIA-ISO and NLIA-STR

NLIA-ISO provides more uniform distribution of axial forces in the columns compared to NLIA-STR. NLIA-STR provides variation of 0.83 to 1.14 times in the axial force compared to NLIA-ISO. The maximum decrease of nearly 0.83 times is found in the corner columns (members 57 to 60) whereas the maximum increase of nearly 1.14 times is found in the inner columns

Table 8 Comparison of bending moment *Mx* (kN-m) in columns for various analyses (*y* = 0 m)

Member No.	Co-ordinates			Case-1 NIA	Case-2 NLIA-ISO	Case-3 NLIA-STR	Comparison of interaction analyses		
	X	Y	Z	1	2	3	2/1	3/1	3/2
57	0.0	0.0	0.0	7.43	-221.80	43.57	-29.87	5.87	-0.20
57	0.0	0.0	2.0	14.04	53.24	42.84	3.79	3.05	0.80
58	0.0	0.0	2.0	21.64	56.98	42.89	2.63	1.98	0.75
58	0.0	0.0	5.5	32.04	71.08	56.59	2.22	1.77	0.80
59	0.0	0.0	5.5	41.54	88.26	66.40	2.12	1.60	0.75
59	0.0	0.0	9.0	40.22	83.38	64.00	2.07	1.59	0.77
60	0.0	0.0	9.0	41.17	91.70	69.81	2.23	1.70	0.76
60	0.0	0.0	12.5	43.71	105.72	78.66	2.42	1.80	0.74
61	6.0	0.0	0.0	10.78	-417.99	46.63	-38.78	4.33	-0.11
61	6.0	0.0	2.0	20.45	105.14	52.70	5.14	2.58	0.50
62	6.0	0.0	2.0	30.91	49.09	56.06	1.59	1.81	1.14
62	6.0	0.0	5.5	45.45	77.87	73.52	1.71	1.62	0.94
63	6.0	0.0	5.5	57.93	110.56	85.89	1.91	1.48	0.78
63	6.0	0.0	9.0	55.75	102.50	82.57	1.84	1.48	0.81
64	6.0	0.0	9.0	56.05	108.39	88.07	1.93	1.57	0.81
64	6.0	0.0	12.5	58.84	123.06	97.51	2.09	1.66	0.79
65	12.0	0.0	0.0	10.80	-489.58	32.37	-45.31	3.00	-0.07
65	12.0	0.0	2.0	20.63	111.28	47.97	5.39	2.32	0.43
66	12.0	0.0	2.0	30.29	44.17	56.06	1.46	1.85	1.27
66	12.0	0.0	5.5	43.90	77.30	72.15	1.76	1.64	0.93
67	12.0	0.0	5.5	55.79	115.37	84.15	2.07	1.51	0.73
67	12.0	0.0	9.0	53.99	106.25	81.26	1.97	1.51	0.76
68	12.0	0.0	9.0	54.79	112.35	87.28	2.05	1.59	0.78
68	12.0	0.0	12.5	57.70	128.17	96.79	2.22	1.68	0.76
69	18.0	0.0	0.0	7.10	-432.26	-0.83	-60.91	-0.12	0.00
69	18.0	0.0	2.0	12.75	124.32	27.73	9.75	2.17	0.22
70	18.0	0.0	2.0	24.18	19.34	45.35	0.80	1.88	2.35
70	18.0	0.0	5.5	38.81	60.30	59.34	1.55	1.53	0.98
71	18.0	0.0	5.5	50.82	101.40	70.00	2.00	1.38	0.69
71	18.0	0.0	9.0	48.09	90.66	66.76	1.89	1.39	0.74
72	18.0	0.0	9.0	47.22	92.97	69.96	1.97	1.48	0.75
72	18.0	0.0	12.5	49.29	106.64	77.01	2.16	1.56	0.72

Note- Negative sign indicates that moment acts in anticlockwise direction about X axis

(members 77 to 80). The maximum compressive force of nearly 1507.00 kN is found in the inner column below plinth level (member 81) of NLIA-ISO. This value of force becomes almost 1.03 times in case of NLIA-STR.

Figs. 6-7 show the variation of axial force in the corner columns (members 57 to 60) and the inner columns (members 77 to 80) of all storeys respectively with load increments for space frame-isolated footing-soil system and space frame-strap footing-soil system. The axial force increases with increase in load increments. The nonlinear variation is found for both the interaction analyses. However, the effect of soil nonlinearity on column axial forces is found to be insignificant.

Table 9 Comparison of bending moment *Mx* (kN-m) in columns for various analyses (*y* = 6 m)

Member No.	Co-ordinates			Case-1 NIA	Case-2 NLIA-ISO	Case-3 NLIA-STR	Comparison of interaction analyses		
	X	Y	Z	1	2	3	2/1	3/1	3/2
73	0.0	6.0	0.0	0.26	6.72	73.55	25.90	283.57	10.95
73	0.0	6.0	2.0	0.29	42.45	39.31	145.55	134.79	0.93
74	0.0	6.0	2.0	-0.85	28.48	11.44	-33.38	-13.41	0.40
74	0.0	6.0	5.5	-1.70	31.00	16.38	-18.20	-9.62	0.53
75	0.0	6.0	5.5	-1.62	35.69	19.95	-22.02	-12.31	0.56
75	0.0	6.0	9.0	-0.80	35.26	19.73	-44.17	-24.71	0.56
76	0.0	6.0	9.0	-0.57	39.81	22.16	-69.90	-38.92	0.56
76	0.0	6.0	12.5	-1.10	45.15	25.04	-41.15	-22.82	0.55
77	6.0	6.0	0.0	0.38	10.17	88.37	26.68	231.87	8.69
77	6.0	6.0	2.0	0.45	59.46	46.54	132.34	103.58	0.78
78	6.0	6.0	2.0	-1.02	29.62	13.21	-28.96	-12.92	0.45
78	6.0	6.0	5.5	-2.09	34.41	19.82	-16.45	-9.48	0.58
79	6.0	6.0	5.5	-1.91	42.76	25.04	-22.41	-13.12	0.59
79	6.0	6.0	9.0	-0.70	42.53	24.95	-60.71	-35.61	0.59
80	6.0	6.0	9.0	0.06	47.75	28.00	839.54	492.27	0.59
80	6.0	6.0	12.5	-0.31	53.45	31.32	-173.19	-101.49	0.59
81	12.0	6.0	0.0	0.31	10.54	89.52	33.69	286.20	8.50
81	12.0	6.0	2.0	0.35	62.35	45.62	177.17	129.63	0.73
82	12.0	6.0	2.0	-1.01	29.20	11.27	-28.92	-11.16	0.39
82	12.0	6.0	5.5	-2.04	33.53	18.05	-16.48	-8.87	0.54
83	12.0	6.0	5.5	-1.86	42.30	23.60	-22.70	-12.67	0.56
83	12.0	6.0	9.0	-0.70	42.30	23.47	-60.69	-33.67	0.55
84	12.0	6.0	9.0	0.02	47.57	26.23	2878.39	1586.70	0.55
84	12.0	6.0	12.5	-0.36	53.03	29.28	-147.41	-81.39	0.55
85	18.0	6.0	0.0	0.64	6.52	78.29	10.15	121.85	12.00
85	18.0	6.0	2.0	0.88	47.31	37.63	53.89	42.87	0.80
86	18.0	6.0	2.0	-1.05	30.24	5.44	-28.78	-5.18	0.18
86	18.0	6.0	5.5	-2.47	28.83	10.73	-11.69	-4.35	0.37
87	18.0	6.0	5.5	-2.70	31.67	15.25	-11.74	-5.65	0.48
87	18.0	6.0	9.0	-1.56	32.55	15.19	-20.85	-9.73	0.47
88	18.0	6.0	9.0	-1.00	38.03	17.25	-38.06	-17.26	0.45
88	18.0	6.0	12.5	-1.52	42.86	19.56	-28.11	-12.83	0.46

Note- Negative sign indicates that moment acts in anticlockwise direction about X axis

5.3 Bending moment (Mx) in the columns

The bending moment (*Mx*) in the columns of frame-footing-soil system due to various analyses is depicted in Tables 8-9 for the total load on the structure.

5.3.1 Effect of soil-structure interaction

The comparison of bending moment due to NIA and NLIA reveals that the interaction effect causes redistribution of the moments in the columns. The significantly higher values of bending moments are found due to NLIA. Also, reversal in the sign takes place in some of the columns.

5.3.2 Effect of inclusion of strap beam

Comparison between NLIA-ISO and NLIA-STR

A very high increase in the bending moment of outer columns (member 57, 61, 65 and 69) is found at the column footing junction in NLIA-ISO as well as reversal in the sign takes place because of the rotation of eccentrically loaded isolated footings. However, NLIA-STR suggests that the use of strap beam controls this moment quite effectively. The use of strap beam decreases the bending moments in most of the columns.

NLIA-STR provides significant variation of -0.20 to 12.00 times in the bending moment compared to NLIA-ISO. The maximum decrease of nearly 0.20 times with reversal in the sign is found in the corner column below plinth level (member 57) whereas the maximum increase of nearly 12.00 times is found in the side column below plinth level (member 85). The maximum

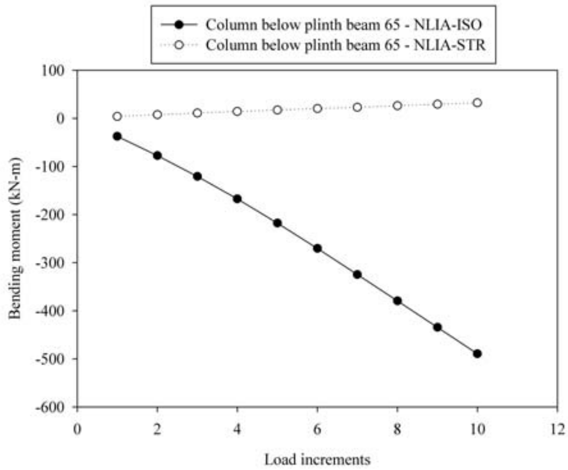

Fig. 8 Comparison of bending moment (*Mx*) at the bottom end of side column (member 65)

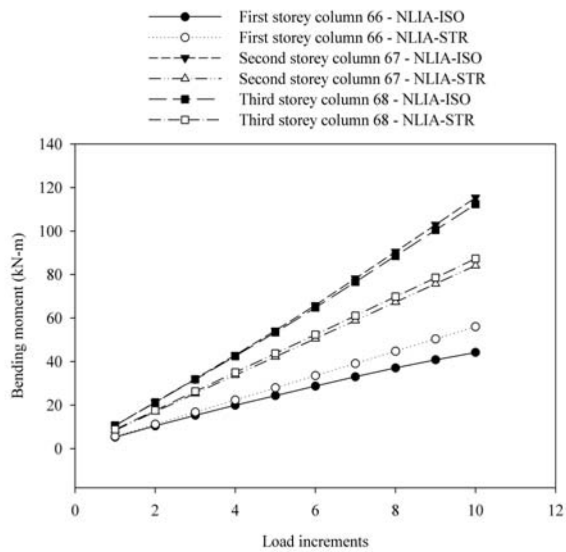

Fig. 9 Comparison of bending moment (*Mx*) at the bottom end of side columns (member 66 to 68)

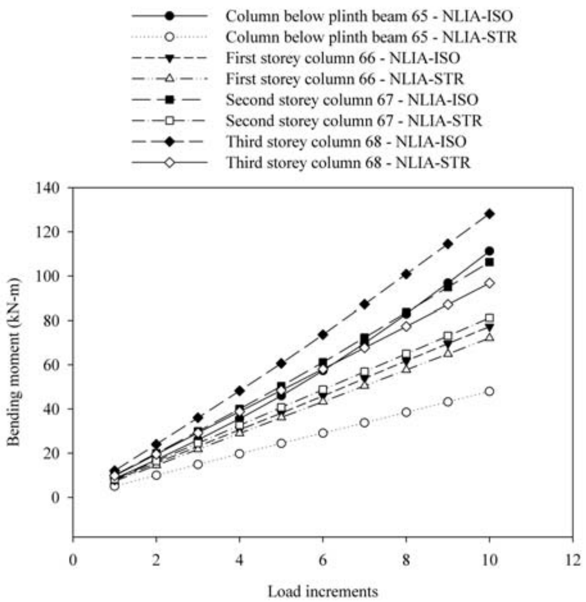

Fig. 10 Comparison of bending moment (*Mx*) at the top end of side columns (members 65 to 68)

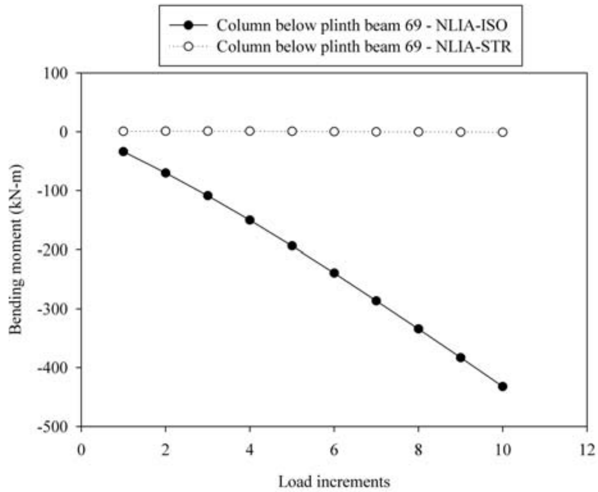

Fig. 11 Comparison of bending moment (*Mx*) at the bottom end of corner column (member 69)

bending moment of nearly -489.58 kN-m is found in the bottom end of side column below plinth level (member 65) of NLIA-ISO. This value of moment becomes almost 0.07 times in case of NLIA-STR accompanied by change in sign.

Figs. 8-13 show the variation of bending moment (*Mx*) in the side columns (members 65 to 68) and the corner columns (members 69 to 72) of all storeys with load increments for space frame-isolated footing-soil system and space frame-strap footing-soil system. The bending moment increases with increase in load increments and nonlinear variation is found for both the interaction analyses. The effect of nonlinearity of soil on column bending moment is found more significant

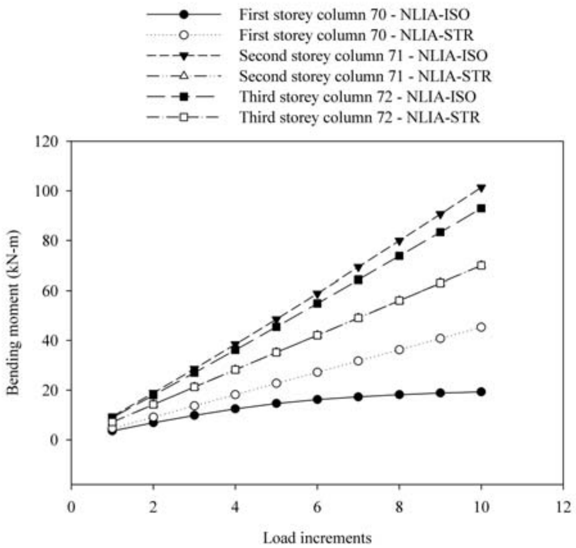

Fig. 12 Comparison of bending moment (*Mx*) at the bottom end of corner columns (members 70 to 72)

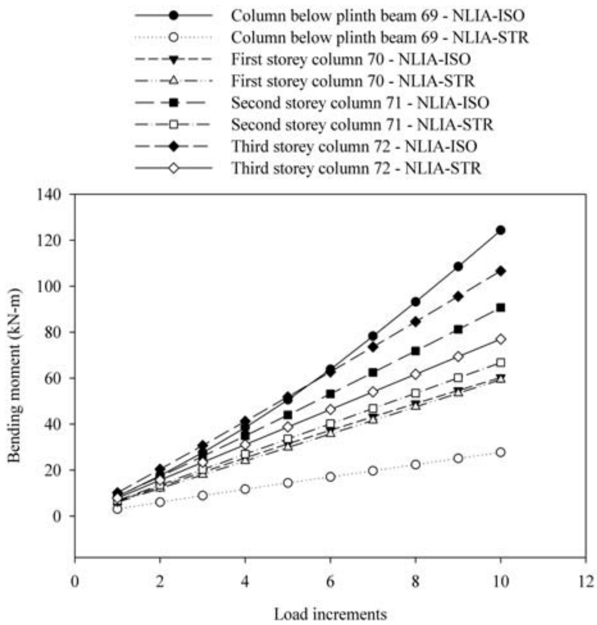

Fig. 13 Comparison of bending moment (*Mx*) at the top end of corner columns (members 69 to 72)

for columns resting on isolated footing compared to the strap footing. The soil nonlinearity causes significant increase in bending moment at the bottom end of side and corner columns resting on eccentric isolated footings whereas less significant effect is found in other columns. The use of strap beam decreases the bending moments in most of the columns.

Table 10 Comparison of bending moment *My* (kN-m) in columns for various analyses (*y* = 0 m)

Member No.	Co-ordinates			Case-1 NIA	Case-2 NLIA-ISO	Case-3 NLIA-STR	Comparison of interaction analyses		
	X	Y	Z	1	2	3	2/1	3/1	3/2
57	0.0	0.0	0.0	154.00	337.64	96.94	2.19	0.63	0.29
57	0.0	0.0	2.0	4.39	86.74	-28.28	19.76	-6.44	-0.33
58	0.0	0.0	2.0	150.23	74.36	132.49	0.49	0.88	1.78
58	0.0	0.0	5.5	116.49	81.26	94.04	0.70	0.81	1.16
59	0.0	0.0	5.5	80.98	22.42	53.64	0.28	0.66	2.39
59	0.0	0.0	9.0	105.91	55.70	81.77	0.53	0.77	1.47
60	0.0	0.0	9.0	21.54	-43.77	-11.70	-2.03	-0.54	0.27
60	0.0	0.0	12.5	57.69	-22.63	17.24	-0.39	0.30	-0.76
61	6.0	0.0	0.0	195.38	83.20	157.47	0.43	0.81	1.89
61	6.0	0.0	2.0	86.77	180.00	72.71	2.07	0.84	0.40
62	6.0	0.0	2.0	246.91	253.93	245.43	1.03	0.99	0.97
62	6.0	0.0	5.5	239.93	261.67	236.03	1.09	0.98	0.90
63	6.0	0.0	5.5	217.99	195.79	208.81	0.90	0.96	1.07
63	6.0	0.0	9.0	230.95	214.67	223.01	0.93	0.97	1.04
64	6.0	0.0	9.0	130.20	108.60	117.15	0.83	0.90	1.08
64	6.0	0.0	12.5	162.28	138.55	148.00	0.85	0.91	1.07
65	12.0	0.0	0.0	196.29	90.95	307.74	0.46	1.57	3.38
65	12.0	0.0	2.0	87.98	265.57	148.69	3.02	1.69	0.56
66	12.0	0.0	2.0	244.87	313.46	262.08	1.28	1.07	0.84
66	12.0	0.0	5.5	235.65	321.68	262.82	1.37	1.12	0.82
67	12.0	0.0	5.5	213.19	262.79	243.23	1.23	1.14	0.93
67	12.0	0.0	9.0	228.15	282.11	257.20	1.24	1.13	0.91
68	12.0	0.0	9.0	128.11	186.07	155.75	1.45	1.22	0.84
68	12.0	0.0	12.5	159.09	226.13	191.67	1.42	1.20	0.85
69	18.0	0.0	0.0	168.60	-333.21	137.76	-1.98	0.82	-0.41
69	18.0	0.0	2.0	31.38	257.41	41.43	8.20	1.32	0.16
70	18.0	0.0	2.0	195.72	153.43	220.27	0.78	1.13	1.44
70	18.0	0.0	5.5	187.41	213.46	209.75	1.14	1.12	0.98
71	18.0	0.0	5.5	172.29	210.93	188.71	1.22	1.10	0.89
71	18.0	0.0	9.0	193.48	229.03	211.47	1.18	1.09	0.92
72	18.0	0.0	9.0	109.02	140.34	126.98	1.29	1.16	0.90
72	18.0	0.0	12.5	149.55	188.97	171.51	1.26	1.15	0.91

Note- Negative sign indicates that moment acts in anticlockwise direction about *Y* axis

5.4 Bending moment (My) in the columns

The bending moment (*My*) in the columns of frame-footing-soil system due to various analyses is depicted in Tables 10-11 for the total load on the structure.

Table 11 Comparison of bending moment *My* (kN-m) in columns for various analyses (*y* = 6 m)

Member No.	Co-ordinates			Case-1 NIA	Case-2 NLIA-ISO	Case-3 NLIA-STR	Comparison of interaction analyses		
	X	Y	Z	1	2	3	2/1	3/1	3/2
73	0.0	6.0	0.0	154.19	444.89	83.54	2.89	0.54	0.19
73	0.0	6.0	2.0	-1.14	79.96	-42.11	-69.92	36.82	-0.53
74	0.0	6.0	2.0	144.18	68.22	124.28	0.47	0.86	1.82
74	0.0	6.0	5.5	116.00	80.69	89.65	0.70	0.77	1.11
75	0.0	6.0	5.5	85.10	18.00	52.63	0.21	0.62	2.92
75	0.0	6.0	9.0	107.64	50.06	78.58	0.47	0.73	1.57
76	0.0	6.0	9.0	19.08	-53.34	-19.54	-2.80	-1.02	0.37
76	0.0	6.0	12.5	53.58	-34.64	6.98	-0.65	0.13	-0.20
77	6.0	6.0	0.0	199.73	76.07	149.35	0.38	0.75	1.96
77	6.0	6.0	2.0	89.64	186.20	67.67	2.08	0.75	0.36
78	6.0	6.0	2.0	249.50	257.58	247.24	1.03	0.99	0.96
78	6.0	6.0	5.5	249.44	272.34	243.34	1.09	0.98	0.89
79	6.0	6.0	5.5	234.12	205.91	221.63	0.88	0.95	1.08
79	6.0	6.0	9.0	245.04	222.93	233.80	0.91	0.95	1.05
80	6.0	6.0	9.0	140.00	112.59	123.62	0.80	0.88	1.10
80	6.0	6.0	12.5	169.82	139.83	151.88	0.82	0.89	1.09
81	12.0	6.0	0.0	200.43	91.36	325.47	0.46	1.62	3.56
81	12.0	6.0	2.0	90.47	305.11	158.83	3.37	1.76	0.52
82	12.0	6.0	2.0	247.38	316.94	271.58	1.28	1.10	0.86
82	12.0	6.0	5.5	245.24	340.42	280.93	1.39	1.15	0.83
83	12.0	6.0	5.5	230.02	290.76	269.59	1.26	1.17	0.93
83	12.0	6.0	9.0	243.32	307.51	281.57	1.26	1.16	0.92
84	12.0	6.0	9.0	139.78	207.79	177.23	1.49	1.27	0.85
84	12.0	6.0	12.5	168.83	246.15	211.78	1.46	1.25	0.86
85	18.0	6.0	0.0	175.83	-471.73	160.88	-2.68	0.91	-0.34
85	18.0	6.0	2.0	40.08	290.61	57.76	7.25	1.44	0.20
86	18.0	6.0	2.0	205.16	164.17	236.04	0.80	1.15	1.44
86	18.0	6.0	5.5	205.39	236.70	235.06	1.15	1.14	0.99
87	18.0	6.0	5.5	198.06	243.10	221.56	1.23	1.12	0.91
87	18.0	6.0	9.0	216.77	258.24	241.41	1.19	1.11	0.93
88	18.0	6.0	9.0	129.45	167.27	155.11	1.29	1.20	0.93
88	18.0	6.0	12.5	169.49	216.29	200.30	1.28	1.18	0.93

Note- Negative sign indicates that moment acts in anticlockwise direction about Y axis

5.4.1 Effect of soil-structure interaction

The comparison of bending moment due to NIA and NLIA reveals that the interaction effect causes redistribution of the moments in the columns. Also, reversal in the sign takes place in some of the columns.

(i) Comparison between NIA and NLIA-ISO

NLIA-ISO provides significant variation of -69.92 to 19.76 times in the bending moment compared to NIA. The maximum decrease of nearly 69.92 times with reversal of sign is found in the side column below plinth level (member 73) whereas the maximum increase of nearly 19.76 times is found in the corner column below plinth level (member 57).

(ii) Comparison between NIA and NLIA-STR

The significant variation of -6.44 to 36.82 times is found in the bending moment due to NLIA-STR compared to NIA. The maximum decrease of nearly 6.44 times with reversal in the sign is found in the corner column below plinth level (member 57) whereas the maximum increase of nearly 36.82 times is found in the side column below plinth level (member 73).

5.4.2 Effect of inclusion of strap beam

Comparison between NLIA-ISO and NLIA-STR

A very high increase in the bending moment of outer columns (member 57, 69, 73 and 85) is found at the column footing junction in NLIA-ISO. However, NLIA-STR suggests that the use of strap beam controls this moment quite effectively. The use of strap beam decreases the bending moments in most of the columns.

NLIA-STR provides significant variation of -0.76 to 3.56 times in the bending moment compared to NLIA-ISO. The maximum decrease of nearly 0.76 times with reversal in sign is found in the corner column of third floor (member 60) whereas the maximum increase of nearly 3.56 times is found in the inner column below plinth level (member 81). The maximum bending moment of nearly -471.73 kN-m is found in the bottom end of side column below plinth level (member 85) of NLIA-ISO. This value of moment becomes almost 0.34 times in case of NLIA-STR accompanied by change in sign.

Figs. 14-19 show the variation of bending moment (*My*) in the side columns (members 73 to 76 and members 85 to 88) of all storeys with load increments for space frame-isolated footing-soil system and space frame-strap footing-soil system. The bending moment increases with increase in load increments and nonlinear variation is found for both the interaction analyses. The effect of nonlinearity of soil on column bending moment is found more significant for columns resting on isolated footing compared to strap footing. The soil nonlinearity causes significant increase in bending moment at the bottom end of the side columns resting on eccentric isolated footings whereas less significant effect is found in other columns. The use of strap beam decreases the bending moments in most of the columns.

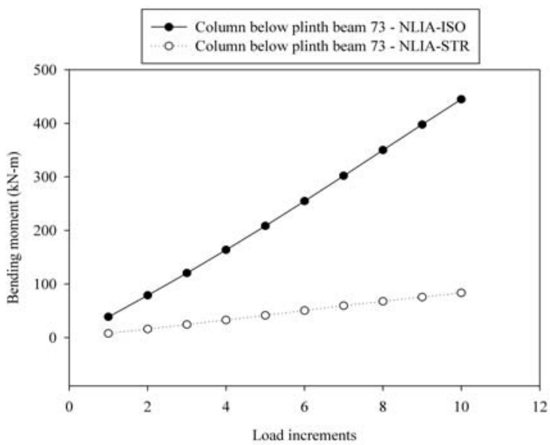

Fig. 14 Comparison of bending moment (*My*) at the bottom end of side column (member 73)

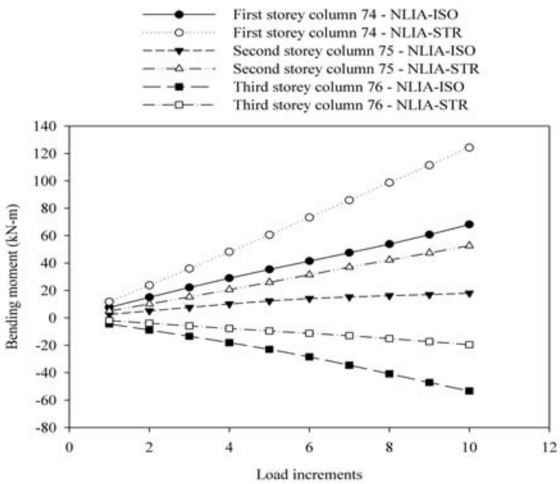

Fig. 15 Comparison of bending moment (*My*) at the bottom end of side columns (members 74 to 76)

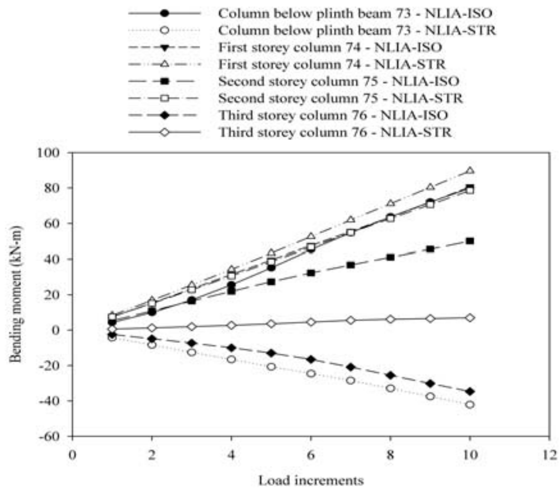

Fig. 16 Comparison of bending moment (*My*) at the top end of side columns (members 73 to 76)

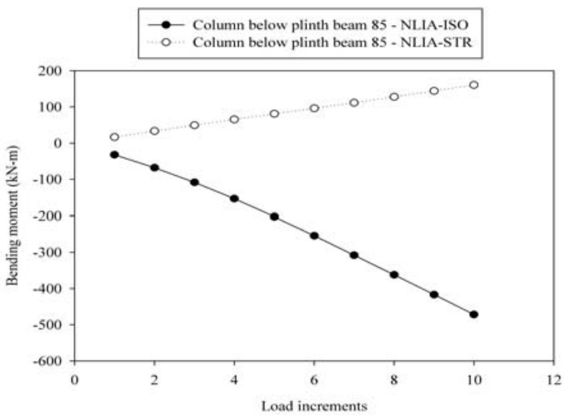

Fig. 17 Comparison of bending moment (*My*) at the bottom end of side column (member 85)

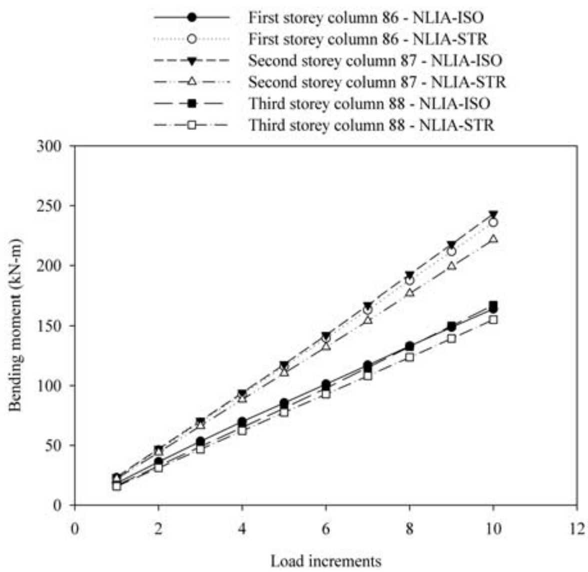

Fig. 18 Comparison of bending moment (*My*) at the bottom end of side columns (members 86 to 88)

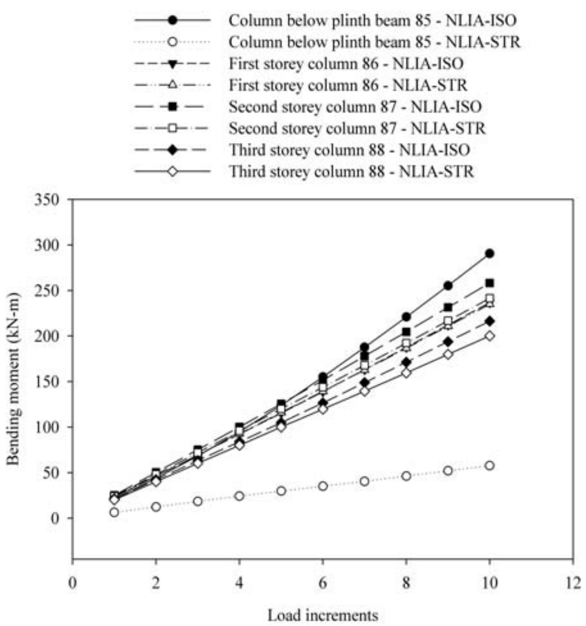

Fig. 19 Comparison of bending moment (*My*) at the top end of side columns (members 85 to 88)

5.5 Shear force (Fx) at column bases

The shear force (*Fx*) at the column bases of frame-footing-soil system due to various analyses is depicted in Table 12 for the total load on the structure.

Table 12 Comparison of shear force *Fx* (kN) at column bases for various analyses

Member No.	Co-ordinates			Case-1 NIA	Case-2 NLIA-ISO	Case-3 NLIA-STR	Comparison of interaction analyses		
	X	Y	Z	1	2	3	2/1	3/1	3/2
57	0.0	0.0	0.0	79.20	208.59	32.50	2.63	0.41	0.16
61	6.0	0.0	0.0	141.07	124.53	111.20	0.88	0.79	0.89
65	12.0	0.0	0.0	142.13	169.80	224.29	1.19	1.58	1.32
69	18.0	0.0	0.0	99.99	-50.88	86.12	-0.51	0.86	-1.69
73	0.0	6.0	0.0	76.52	257.78	17.69	3.37	0.23	0.07
77	6.0	6.0	0.0	144.68	121.24	102.87	0.84	0.71	0.85
81	12.0	6.0	0.0	145.45	186.07	236.50	1.28	1.63	1.27
85	18.0	6.0	0.0	107.96	-108.74	104.45	-1.01	0.97	-0.96

5.5.1 Effect of soil-structure interaction

The comparison of shear force due to NIA and NLIA reveals that the interaction effect causes significant redistribution of the shear forces at column bases. This redistribution of shear forces is more significant in case of NLIA-ISO compared to NLIA-STR.

(i) Comparison between NIA and NLIA-ISO

NLIA-ISO provides significant variation of -1.01 to 3.37 times in the shear force compared to NIA. The maximum decrease of nearly 1.01 times alongwith reversal of sign is found at the base of side column (member 85) whereas the maximum increase of nearly 3.37 times is found at the base of side column (member 73). The maximum shear force of nearly 145.45 kN is found at the base of inner column (member 81) in case of NIA. This value of shear force becomes almost 1.28 times in case of NLIA-ISO.

(ii) Comparison between NIA and NLIA-STR

The significant variation of 0.23 to 1.63 times is found in the shear force due to NLIA-STR compared to NIA. The maximum decrease of nearly 0.23 times is found at the base of side column (member 73) whereas the maximum increase of nearly 1.63 times is found at the base of inner column (member 81). The maximum shear force of nearly 145.45 kN is found at the base of inner column (member 81) in case of NIA. This value of shear force becomes almost 1.63 times in case of NLIA-ISO.

5.5.2 Effect of inclusion of strap beam

Comparison between NLIA-ISO and NLIA-STR

The inclusion of strap beam causes decrease in the shear force in most of the column bases compared to NLIA-ISO. Also, reversal in the sign takes place in some of the columns. NLIA-STR provides variation of -1.69 to 1.32 times in the shear force compared to NLIA-ISO. The maximum decrease of nearly 1.69 times is found at the base of corner column (member 69) whereas the maximum increase of nearly 1.32 times is found at the base of side column (member 65). The maximum shear force of nearly 257.78 kN is found at the base of side column (member 73) of NLIA-ISO. This value of force becomes almost 0.07 times in case of NLIA-STR.

5.6 Shear force (Fy) at column bases

The shear force (*Fy*) at the column bases of frame-footing-soil system due to various analyses is depicted in Table 13 for the total load on the structure.

Table 13 Comparison of shear force *Fy* (kN) at column bases for various analyses

Member No.	Co-ordinates			Case-1 NIA-S	Case-2 NLIA-ISO	Case-3 NLIA-STR	Comparison of interaction analyses		
	X	Y	Z	1	2	3	2/1	3/1	3/2
57	0.0	0.0	0.0	-10.73	85.15	-43.22	-7.93	4.03	-0.51
61	6.0	0.0	0.0	-15.62	160.06	-49.71	-10.25	3.18	-0.31
65	12.0	0.0	0.0	-15.72	194.04	-40.20	-12.34	2.56	-0.21
69	18.0	0.0	0.0	-9.92	158.68	-13.44	-15.99	1.35	-0.08
73	0.0	6.0	0.0	-0.28	-24.44	-56.46	88.73	204.94	2.31
77	6.0	6.0	0.0	-0.42	-34.32	-67.52	82.66	162.62	1.97
81	12.0	6.0	0.0	-0.33	-35.86	-67.63	107.88	203.50	1.89
85	18.0	6.0	0.0	-0.76	-26.70	-58.00	35.12	76.29	2.17

5.6.1 Effect of soil-structure interaction

The comparison of shear force due to NIA and NLIA reveals that the interaction effect causes significant redistribution of the forces at column bases. The significantly higher values of shear force is found due to NLIA. Also, reversal in the sign takes place in some of the columns.

5.6.2 Effect of inclusion of strap beam

Comparison between NLIA-ISO and NLIA-STR

The NLIA-STR causes significant decrease in the higher values of shear force at the column bases compared to NLIA-ISO. Also, reversal in the sign takes place in some of the columns. NLIA-STR provides variation of -0.51 to 2.31 times in the shear force compared to NLIA-ISO. The maximum decrease of nearly 0.51 times with reversal in the sign is found at the base of corner column (member 57) whereas the maximum increase of nearly 2.31 times is found at the base of side column (member 73). The maximum shear force of nearly 194.04 kN is found at the base of side column (member 65) of NLIA-ISO. This value of shear force becomes almost 0.21 times in case of NLIA-STR accompanied by change in sign.

6. Conclusions

Based on the findings of the present study, the following conclusions are made:

· The interaction effect causes significant redistribution of forces and moments in the column members.

· The soil nonlinearity causes significant increase in bending moment at the bottom end of columns resting on eccentric isolated footings whereas less significant effect is found in other columns.

· The forces in the column members are found to vary nonlinearly with load increments.

· The axial forces in the columns are distributed more uniformly when interaction effects are considered in the analysis. The heavily loaded inner columns are relieved of the axial forces and corresponding increase is found in the corner columns.

· The bending moments of very high magnitude are induced at column bases resting on eccentric footing of frame-isolated footing-soil interaction system. However, use of strap beams controls these moments quite effectively.

· The use of strap beam decreases the bending moments in most of the columns.

· The inclusion of strap beam causes significant decrease in the higher values of shear force in most of the column bases resting on isolated footing.

· The inclusion of strap beam significantly decreases the foundation settlements.

References

Abdullah, W.S. (2011), "Viscoplastic finite element analysis of complex geotechnical problems", *Jordan J. Eng.*, **5**(2), 302-314.

Agrawal, R. and Hora, M.S. (2012), "Nonlinear interaction behaviour of plane frame-layered soil system subjected to seismic loading", *Int. J. Struct. Eng. Mech.*, **41**(6), 711-734.

Agrawal, R. and Hora, M.S. (2012), "Nonlinear interaction behaviour of infilled frame-isolated footings-soil system subjected to seismic loading", *Int. J. Struct. Eng. Mech.*, **44**(1), 85-107.

Asteris, P.G. (2003), "Lateral stiffness of brick masonry infilled plane frames", *J. Struct. Eng.*, ASCE, **129**(8), 1071-1079.

Asteris, P.G., Antoniou, S.T., Sophianopoulos, D.S. and Chrysostomou, C.Z. (2011), "Mathematical macromodeling of infilled frames: state of the art", *J. Struct. Eng.*, ASCE, **137**(12), 1508-1517.

Asteris, P.G. and Cotsovos, D.M. (2012), "Numerical investigation of the effect of infill walls on the structural response of RC frames", *The Open Construction and Building Technology Journal*, Bentham Science Publishers, **6**, 164-181.

Al-Shamrani, M.A. and Al-Mashary, F.A. (2003), "A simplified computation of the interactive behavior between soils and framed structures", *Eng. Sci*., **16**(1), 37-60.

Bhattacharya, K., Dutta, S.C. and Roy, R. (2006), "Seismic design aids for buildings incorporating soil-flexibility effect", *J. Asian Archit. Build*., **5**(2), 341-348.

Bishop, A.W. and Henkel, D.J. (1957), *The measurement of soil properties in the triaxial test*, Edward Arnold Ltd., London.

Buragohain, D.N. and Shah, V.L. (1979), "Three dimensional interactive finite element analysis of foundation structures", *Proceedings of international conference on computer application civil engineering*, Roorkee, India.

Chore, H.S., Ingle, R.K. and Sawant, V.A. (2010) "Building frame-pile foundation-soil interaction analysis: a parametric study", *J. Interact. Multiscale Mech.*, **3**(1), 55-79.

Chrysostomou, C.Z. and Asteris, P.G. (2012), "On the in-plane properties and capacities of infilled frames", *Eng. Struct.*, **41**, 385-402.

Desai, C.S., Phan, H.V. and Perumpral, J.V. (1982), "Mechanics of three-dimensional soil-structure interaction", *J. Eng. Mech., ASCE*, **108**(5), 731-747.

Duncan, J.M. and Chang, C.Y. (1970) "Nonlinear analysis of stress and strain in soils", *J. Soil Mech. Found. Eng. Div. ASCE*, **96**(5), 1629-1653.

Dutta, S.C. and Roy, R. (2002), "A critical review on idealization and modeling for interaction among soil-foundation-structure system", *Comput. Struct.*, **80**, 1579-1594.

French, S.E. (1999), *Design of Shallow Foundations*, ASCE Press, USA.

Guzman, T. (2010), "Heavily loaded strap footing-design, detailing and behavior", *Structure Magazine*, 12-15.

Hora, M. (2006), "Nonlinear interaction analysis of infilled building frame-soil system", *J. Struct. Eng.*, **33**(4), 309-318.

Jardine, R.J., Potts, D.M., Fourie, A.B. and Burland, J.B. (1986), "Studies of the influence of non-linear stress-strain characteristics in soil-structure interaction", *Geotechnique*, **36**(3), 377-396.

Kondner, R.L. (1963), "Hyperbolic stress-strain response: cohesive soils", *J. Soil Mech. Found. Eng. Div., ASCE*, **89**(SM1), 115-144.

Kutanis, M. and Elmas, M. (2001), "Non-linear seismic soil structure interaction analysis based on the substructure method in the time domain", *Turk. J. Eng. Environ. Sci.*, **25**, 617-626.

Lu, X., Chen, B., Li, P. and Chen, Y. (2003), "Numerical analysis of tall buildings considering dynamic soil-structure interaction", *J. Asian Archit. Build.*, **2**(1), 1-8.

Mandal, A., Moitra, D. and Dutta, S.C. (1998), "Soil-structure interaction on building frame: a small scale model study", *Int. J. Struct.*, **18**(2), 92-108.

Moghaddam, H.A. and Dowling, P.J. (1987), "The state-of-art in infilled frames", *ESEE Research Report No. 87-2*, Imperial college of Science and Technology, London, U.K.

Nataralan, K. and Vidivelli, B. (2009), "Effect of column spacing on the behavior of frame-raft and soil systems", *J. Appl. Sci.*, **9**(20), 3629-3640.

Noorzaei, J. (1991), "Non-Linear soil–structure interaction in framed structures", Ph.D. Dissertation, University of Roorkee, Roorkee.

Noorzaei J., Viladkar, M.N. and Godbole, P.N. (1994), "Nonlinear soil-structure interaction in plane frames", *Eng. Comput.*, **11**, 303-316.

Noorzaei, J. (1996), "Concepts and application of three dimensional infinite elements to soil-structure-interaction problems", *Int. J. Eng*., **9**(3), 131-142.

Pender, M.J., Wotherspoon, L.M., Ingham, J.M. and Carr, A.J. (2006), "Shallow foundation stiffness: continuous soil and discrete spring models compared", *Proceedings of NZSEE Conference*, New Zealand.

Roy, R. and Dutta, S.C. (2001), "Differential settlement among isolated footings of building frames: the problem, its estimation and possible measures", *Int. J. Appl. Mech. Eng.*, **6**(1), 165-186.

Swamy Rajashekhar, H.M., Krishnamoorthy, Prabakhara, D.L. and Bhavikatti, S.S. (2011), "Relevance of interface elements in soil structure interaction analysis of three dimensional and multiscale structure on raft foundation", *Electron. J. Geotech. Eng.*, **16**, 199-218.

Swanson, J.A., ANSYS-Engineering Analysis Systems User's Manual, Swanson Analysis Systems, Inc., Johnson Rd., P.O. Box 65, Houston, PA 15342.

Thangaraj, D. and Ilamparuthi, K. (2010), "Parametric study on the performance of raft foundation with interaction of frame", *Electron. J. Geotech. Eng.*, **15**, 861-878.

Thangaraj, D. and Ilamparuthi, K. (2012), "Numerical analyses of soil-mat foundation and space frame system", *J. Interact. Multiscale Mech.*, **5**(3), 266-286.

Varghese, P.C. (2006), *Foundation Engineering*, Prentice-Hall of India Pvt. Ltd., India.

Viladkar, M.N., Ranjan, G. and Sharma, R.P. (1993), "Soil-structure interaction in the time domain", *Comput. Struct.*, **46**(3), 429-442.

Viladkar, M.N., Noorzaei, J. and Godbole, P.N. (1994) "Interactive analysis of a space frame-raft-soil system considering soil nonlinearity", *Comput. Struct.*, **51**, 343-356.

Wang, C.M., Chow, Y.K. and How, Y.C. (2001) "Analysis of rectangular thick rafts on an elastic half-space", *Comput. Geotech.*, **28**(3), 161-184.